Supporting Information

Tertiary amine ionic liquid incorporated Fe_3O_4 nanoparticles as a versatile catalyst for the Knoevenagel reaction

Xiaoli Jia [a], Xiaoyu Zhang [b], Zhijun Wang [c] and Sanhu Zhao [a]*

[a] *Department of Chemistry, Xinzhou Teachers University, Xinzhou 034000, China.*

[b] *School Chemistry and Material Science, Shanxi Normal University, Linfen 041001, China.*

[c] *Department of Chemistry, Changzhi University, Changzhi 046011, China.*

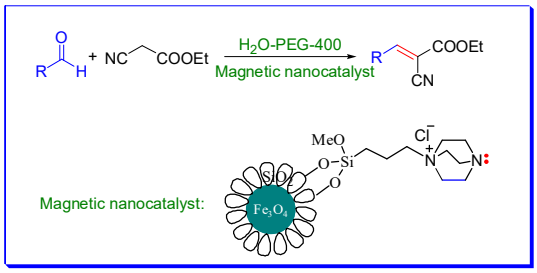

Contents

1. Structure characterization of the magnetic nanocatalyst(MNPs)

FTIR analysis

To investigate the functional group and the structure of the MNPs, the FTIR spectroscopy was conducted and the results are shown in Figure 1. As can be seen from the infrared spectra of the four kinds of nanoparticles, the peak at 572 cm^{-1} is the stretching vibration absorption peak of the Fe-O bond.[1] The peak at 3435 cm^{-1} indicates the presence of hydroxyl groups on the surface of the catalyst. The peaks at 1082 cm^{-1}, 778 cm^{-1} and 472 cm^{-1} in Figure 1 (curve **b**, **c** and **d**) is the stretching vibration peak of the Si-O bond. the peaks at 2997 cm^{-1} and 2910 cm^{-1} (Figure 1, curve **c** and **d**) are the stretching vibration of C-H bond. The stretching vibration of C-N bond was observed at 1620 cm^{-1} (Figure 1, curve **d**). All these signs indicate that DABCO had successfully adhered to the magnetic nanoparticles.

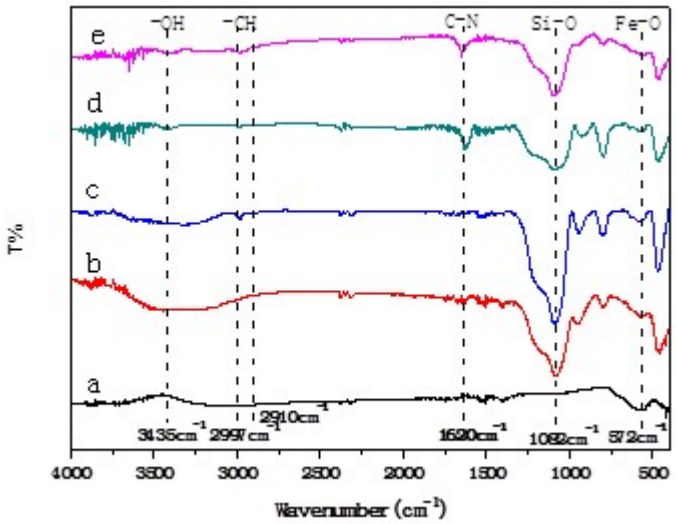

a. Fe_3O_4 b. Fe_3O_4@SiO_2 c. Fe_3O_4@SiO_2@propylchloride d. Fe_3O_4@SiO_2@propyl@DABCO e. Fe_3O_4@SiO_2@propyl@DABCO after 8th run.

Fig. 1 FTIR spectra of nanoparticles. E.

XRD analysis

In order to analyze the crystal structure and composition of magnetic nanoparticles Fe_3O_4, Fe_3O_4@SiO_2, Fe_3O_4@SiO_2@propylchloride and Fe_3O_4@SiO_2@propyl@DABCO, X-ray diffraction (XRD) was further studied. As shown in the diffraction diagram (Figure 2), the diffraction peaks 220, 311, 400, 422, 511, 440 at 2θ = 30.3°, 35.678°, 43.34°, 53.08°, 57.22°, 62.8° are the characteristic

peaks of the standard Fe_3O_4. These peaks are present in the XRD patterns of each particles, which indicate that Fe_3O_4 has a cubic spinel structure and its surface modification does not cause phase transition.[2] The board peak at 18°-28° indicates that there is amorphous silicon sell on the surface of Fe_3O_4. In addition, the Debye-Scherrer equation(D= $K\lambda/\beta\cos\theta$, where D is crystal diameter, K is 0.89, λ is the wavelength of X-ray, β is the full width at half maximum of the peak in radians, and θ is the Bragg diffraction angle in radians) was used to calculate the particle size of final magnetic nanoparticle. For the particle of Fe_3O_4, 2θ = 35.678, β = 0.598, D = 16.3 nm, the particle of Fe_3O_4@SiO_2, 2θ = 35.64, β = 0.754, D = 12.9 nm, the particle of Fe_3O_4@SiO_2@propylchloride, 2θ = 35.58, β = 0.696, D = 14.0 nm and the particle of Fe_3O_4@SiO_2@propyl@DABCO, 2θ = 35.839, β = 0.63, D = 15.51 nm. The calculation results showed that the average grain size of the final magnetic nanocatalyst is 15.51 nm, which is similar to the results obtained by TEM and SEM analysis.

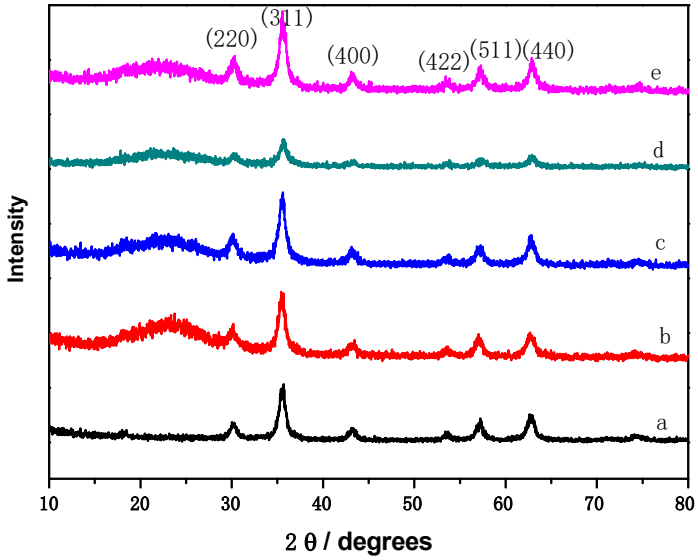

a. Fe_3O_4 b. Fe_3O_4@SiO_2 c. Fe_3O_4@SiO_2@propylchloride d. Fe_3O_4@SiO_2@propyl@DABCO

Fig. 2 XRD patterns of nanoparticles.

TEM analysis

Then, the morphology and crystal structure of the Fe_3O_4@SiO_2@propyl@DABCO nanoparticles were analyzed by transmission electron microscopy (TEM). As can be seen from Figure 3, the magnetic nanoparticles are spherical, and the particle size can be

observed in the range of 10-20 nm, which is similar to the results obtained by Scherrer formula. Combined with XRD analysis, it can be preliminarily inferred that the surface of Fe_3O_4 is covered with SiO_2, propyl group and DABCO.

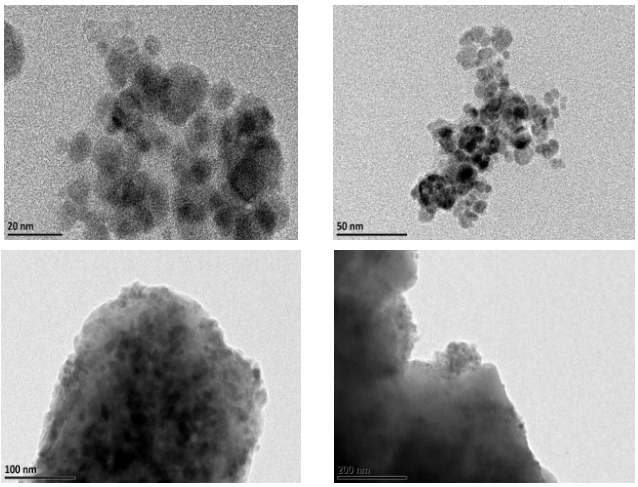

Fig. 3 TEM images of Fe_3O_4@SiO_2@propyl@DABCO nanoparticles.

SEM analysis

Figure 4 displays the SEM image of Fe_3O_4@SiO_2@propyl@DABCO, it can be found that the shape of the magnetic nanocatalyst is spherical and the size of the nanoparticles is between 10 and 15 nm, which is consistent with the TEM analysis. In addition, it can be observed from Figure 4 that some particles appear agglomeration, which should be caused by the magnetic effect.

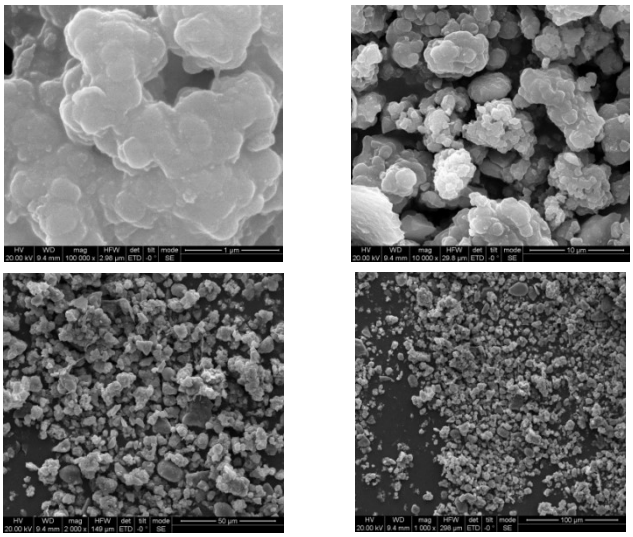

Fig. 4 SEM images of Fe_3O_4@SiO_2@propyl@DABCO nanoparticles.

TG analysis

In order to study the thermal stability and the structure of the Fe_3O_4@SiO_2@propyl@DABCO nanoparticles, thermo gravimetric analysis (TG) was performed at temperatures ranging from 30 ºC to 1000 ºC. As shown in the Figure 5, there are three distinct stages of mass loss. The mass loss 3.37% at 30-210 ºC may be caused by the evaporation of water or residual solvent on the surface of the catalyst. A mass loss of approximately 5.90% in the second stage between 210 ºC and 610 ºC was attributed to the loss of propyl group and DABCO. In the third stage at 610-1000 ºC, the mass loss is about 2.02%, which may be attributed to the decomposition of the silicon shell. From the analysis of three stages of thermo gravimetric data, the preparation of DABCO nanocatalyst supported in the form of ionic salt is successful.

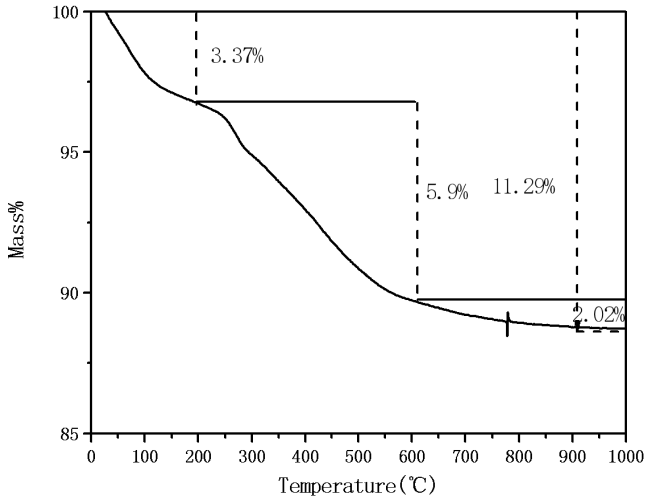

Fig. 5 TG curve of Fe_3O_4@SiO_2@propyl@DABCO nanoparticles.

BET analysis

To better understand the mechanism of action of the catalyst Fe_3O_4@SiO_2@propyl@DABCO, the pore volume, specific surface area and pore diameter of the catalyst were determined by BET test, the results are as in Figure 6. The specific surface area of the catalyst is 1.0936 m^2/g, the pore volume is 0.003349 cm^3/g and the average pore diameter is 13.1134 nm. The loop between 0.45 and 0.95 indicates that the catalyst has a mesoporous structure, the mesoporous structure of the catalyst is favorable for the interaction between the catalytic site and the reaction molecules, which can also be seen from the experimental results.

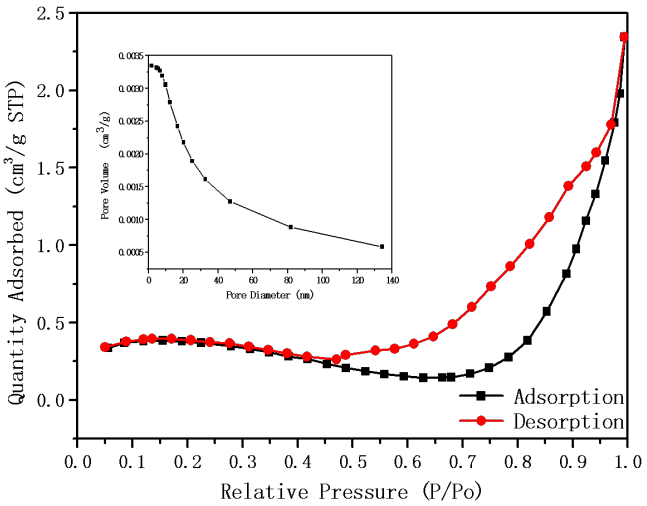

Fig. 6 N_2 adsorption/desorption and pore size distribution curve.

VSM analysis

Finally, magnetic measurement of the magnetic nanoparticles Fe_3O_4@SiO_2@propyl@DABCO was also carried out through the vibrating sample magnetometer (VSM). As can be seen from Figure 7, not only the nanoparticles showed good paramagnetism and dispersive properties in water, but under the action of external magnetic field, the nanoparticles showed good aggregation, which provides support for its recycling in water phase.

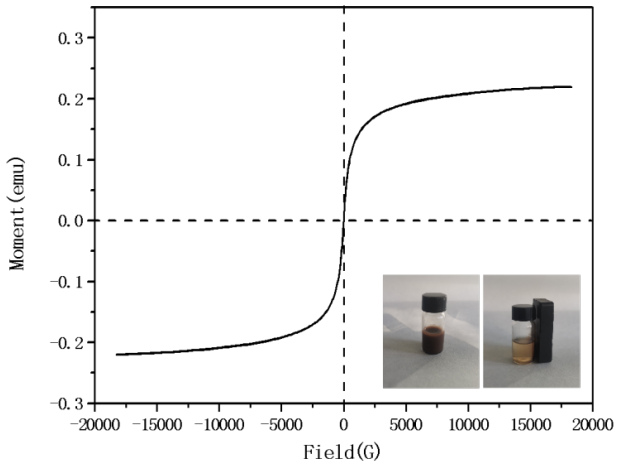

Fig. 7 VSM image of Fe_3O_4@SiO_2@propyl@DABCO particles.

2. Spectral data of Knoevenagel products

Ethyl-3-(4-chlorophenyl)-2-cyanoacrylate (Table 2, Entry 1)

White crystal; m.p. 92.5-93.1 °C (Lit.[3] 92.8-93.2 °C). ^{1}H NMR (400 MHz, $CDCl_3$) δ 8.18 (s, 1H, CH=), 7.92 (d, J = 8.4 Hz, 2H, ArH), 7.46 (d, J = 8.4 Hz, 2H, ArH), 4.38 (q, J = 7.1 Hz, 2H, CH_2), 1.39 (t, J = 7.1 Hz, 3H, CH_3). ^{13}C NMR (101 MHz, $CDCl_3$) δ 162.15, 153.27, 139.50, 132.18, 129.89, 129.63, 115.22, 103.53, 62.83, 14.13.

Ethyl-2-cyano-3-(4-nitrophenyl)acrylate (Table 2, Entry 2)

Yellow solid; m.p. 169.8-170.4 °C (Lit.[3] 170.2–170.8 °C). ^{1}H NMR (400 MHz, $CDCl_3$) δ 8.36 (d, J = 8.8 Hz, 2H, ArH), 8.33 (s, H, CH=), 8.16 (d, J = 8.8 Hz, 2H, ArH), 4.45 (q, J = 7.1 Hz, 2H, CH_2), 1.44 (t, J = 7.1 Hz, 3H, CH_3).

Ethyl-2-cyano-3-(4-hydroxyphenyl)acrylate (Table 2, Entry 3)

Yellow solid; m.p. 171.2-171.8 °C (Lit.[3] 171.5-171.8 °C). ^{1}H NMR (400 MHz, DMSO-d_6) δ 10.83 (s, 1H, OH), 8.24 (s, 1H, CH=), 8.00 (d, J = 8.3 Hz, 2H, ArH), 6.95 (d, J = 8.3 Hz, 2H, ArH), 4.29 (q, J = 7.0 Hz, 2H, CH_2), 1.29 (t, J = 7.0 Hz, 3H, CH_3). ^{13}C NMR (101 MHz, DMSO-d_6) δ 163.32, 163.03, 155.10, 134.40, 122.95, 116.88, 116.81, 97.51, 62.38, 14.48.

Ethyl-2-cyano-3-(4-fluorophenyl)acrylate (Table 2, Entry 4)

White solid; m.p. 97.6- 97.9°C (Lit.[3] 97.8-98.1 °C). ^{1}H NMR (400 MHz, $CDCl_3$) δ 8.22 (s, 1H, CH=), 8.05 (t, J = 7.7 Hz, 2H, ArH), 7.21 (t, J = 7.7 Hz, 2H, ArH), 4.39 (q, J = 7.1 Hz, 2H, CH_2), 1.41 (t, J = 7.1 Hz, 3H, CH_3).

Ethyl-2-cyano-3-(4-cyanophenyl)acrylate (Table 2, Entry 5)

White crystal solid; m.p. 169.2-169.7 °C (Lit.[3] 168.7–169.4 °C). ^{1}H NMR (400 MHz, $CDCl_3$) δ 8.25 (s, 1H, CH=), 8.07 (d, J =8.4 Hz, 2H, ArH), 7.80 (d, J =8.3 Hz, 2H, ArH), 4.42 (q, J =6.8 Hz, 2H, CH2), 1.42 (t, J = 7.5 Hz, 3H, CH_3).

Ethyl 2-cyano-3-(4-methoxy-phenyl)acrylate (Table 2, Entry 6)

Pale yellow crystal solid; m.p. 82.2-82.7 °C (Lit.[3] 81.8-82.5 °C). ^{1}H NMR (400 MHz, $CDCl_3$) δ 8.17 (s, 1H, CH=), 8.01 (d, J = 8.8 Hz, 2H, ArH), 7.00 (d, J = 8.9 Hz, 2H, ArH), 4.37 (q, J = 7.1 Hz, 2H, CH_2), 3.9 (s, 3H, OCH_3), 1.40 (t, J = 7.1 Hz, 3H, CH_3).

Ethyl-2-cyano-3-(4-phenylphenyl)acrylate (Table 2, Entry 7)

Green solid; m.p. 121.5-121.9 °C (Lit.[4] 121.8 °C). ^{1}H NMR (400 MHz, DMSO-d_6) δ 8.45 (s, 1H,CH=), 8.17 (d, J = 8.0 Hz, 2H, ArH), 7.93 (d, J = 8.0 Hz, 2H, ArH), 7.80 (d, J = 7.6 Hz, 2H, ArH), 7.54-7.45 (m, 3H, ArH), 4.34 (q, J = 7.0 Hz, 2H, CH_2), 1.32 (t, J = 7.0 Hz, 3H, CH_3). ^{13}C NMR (101 MHz, DMSO-d_6) δ 162.34, 154.87, 145.13, 138.91, 132.03, 130.78, 129.57, 129.11, 127.80, 127.43,116.29, 102.40, 62.80, 14.30.

Diethyl-3, 3'-(1, 4-phenylene)-bis(2-cyanoacrylate) (Table 2, Entry 8)

White crystal solid; m.p. 187.5-188.1 °C (Lit. [3] 187.8-188.3 °C). ^{1} H-NMR (400 MHz, $CDCl_3$) δ 8.27 (s, 2H, CH=), 8.11 (s, 4H, ArH), 4.42 (q, J = 7.1 Hz, 4H, CH_2), 1.42 (t, J =7.1 Hz, 6H, CH_3).

Ethyl-2-cyano-3-(2, 4-dichlorophenyl)acrylate(Table 2, Entry 9)

White solid; m.p. 82.4-82.8 °C (Lit.[3] 82.6-82.9 °C). ^{1}H NMR (400 MHz, $CDCl_3$) δ 8.63 (s, 1H,CH=), 8.23 (d, J = 8.6 Hz, 1H, ArH), 7.55 (d, J = 1.9 Hz, 1H, ArH), 7.42 (d, J = 8.6 Hz, 1H, ArH), 7.29 (s, 2H), 4.43 (q, J = 7.1 Hz, 2H,CH_2), 1.43 (t, J = 7.1 Hz, 3H,CH_3).

Ethyl-2-cyano-3-phenylacrylate (Table 2, Entry 10)

White crystal solid; m.p. 51.7-52.2 °C (Lit.[3] 50.8–51.3 °C). ^{1}H NMR (400 MHz, $CDCl_3$) δ 8.26 (s, 1H, CH=), 8.00-7.99 (m, 2H, ArH), 7.57-7.49 (m, 3H, ArH), 4.41 (q, J = 7.1 Hz, 2H, CH_2), 1.41 (t, J = 7.1 Hz, 3H, CH_3).

Ethyl 2-cyano-3-anthracenylacrylate (Table 2, Entry 11)

Yellow solid; m.p. 188.2-188.8 °C (Lit.[3] 187.8-188.3 °C). ^{1}H NMR (400 MHz, DMSO-d_6) δ 9.41 (s, 1H,CH=), 8.89 (s, 1H, ArH), 8.27 (d, J = 7.9 Hz, 2H, ArH), 8.60 (d, J = 8.2 Hz, 2H, ArH), 7.70 (t, J = 7.3 Hz, 4H, ArH), 4.49 (q, J = 6.9 Hz, 2H, CH_2), 1.45 (t, J = 6.9 Hz, 3H, CH_3). ^{13}C NMR (151 MHz, DMSO-d_6) δ 161.17, 155.79, 130.80, 130.44, 129.43, 128.67, 127.78, 126.44, 125.33, 123.82, 114.82, 113.90, 62.98, 14.45.

Ethyl-2-cyano-3-(2, 4-dimethoxyphenyl)acrylate (Table 2, Entry 12)

Yellow crystal solid; m.p. 139.8-140.3 °C (Lit.[5] 138-139 °C). ^{1}H NMR (400 MHz, DMSO-d_6) δ 8.52 (s, 1H, CH=), 8.22 (d, J = 8.9 Hz, 1H, ArH), 6.77 (d, J = 9.0 Hz, 1H, ArH), 6.73 (s, 1H, ArH), 4.29 (q, J = 7.0 Hz, 2H, CH_2), 3.91 (d, J = 11.2 Hz, 6H. OCH_3), 1.29 (t, J = 7.0 Hz, 3H, CH_3). ^{13}C NMR (151 MHz, DMSO-d_6) δ 166.07,

163.12, 161.79, 148.15, 130.48, 117.00, 113.16, 107.74, 98.76, 97.81, 62.41, 56.78, 56.40, 14.48.

Ethyl-2-cyano-3-(2-methoxyphenyl)acrylate (Table 2, Entry 13)

Light green solid; m.p. 73.2- 73.8°C (Lit.[6] 72-74 °C). ^{1}H NMR (60 MHz, $CDCl_3$) δ 8.80 (s, 1H, CH=) 8.34 (d, J = 7.4 Hz, 1H, ArH), 7.53 (d, J = 7.3 Hz, 1H, ArH), 7.09 (t, J = 7.5 Hz, 2H, ArH), 4.55-4.13 (m, 2H, CH_2), 3.97 (s, 3H, OCH_3), 1.46 (t, J = 6.8 Hz, 3H, CH_3). ^{13}C NMR (15 MHz, $CDCl_3$) δ 163.14, 159.07, 149.42, 134.76, 129.12, 120.74, 115.94 , 111.10, 102.58, 62.24, 55.62, 14.59.

Ethyl 2-cyano-3-(furan-2-yl)acrylate(Table 2, Entry 14)

Light yellow needle crystals; m.p. 96.8-97.1 °C (Lit.[3] 96.6–97.2 °C). ^{1}H NMR (400 MHz, $CDCl_3$) δ 8.04 (s, 1H, -Fur-H), 7.77 (s, 1H, =CH), 7.40 (s, 1H, -Fur-H), 6.69 (s, 1H, -Fur-H), 4.38 (q, J = 7.1 Hz, 2H, CH_2), 1.40 (t, J = 7.1 Hz, 3H, CH_3).

Ethyl 2-cyano-3-(*N*-ethylcarbazol-3-yl) acrylate (Table 2, Entry 15)

Yellow crystals; m.p. 141.8-142.5 °C (Lit.[4] 142 °C). ^{1}H NMR (400 MHz, $CDCl_3$) δ 8.70 (s, 1H, ArH), 8.39 (s, 1H, =CH), 8.17 (dd, J = 21.2, 8.1 Hz, 2H, ArH), 7.43 (dt, J = 28.3, 21.0 Hz, 4H, ArH), 4.40 (td, J = 14.2, 7.0 Hz, 4H, $2CH_2$), 1.46 (dd, J = 16.4, 7.3 Hz, 6H, $2CH_3$).

2-(4-chlorobenzylidene) malononitrile (Table 2, Entry 16)

White solid; m.p. 163.8-164.3 °C (Lit.[7] 164 °C). ^{1}H NMR (400 MHz, $CDCl_3$) δ 7.88 (d, J = 8.2 Hz, 2H, ArH), 7.77 (s, 1H, =CH), 7.54 (d, J = 8.3 Hz, 2H, ArH).

3-(4-nitrobenzylidene)malononitrile(Table 2, Entry 17)

Yellow solid; m.p. 161.4-161.9 °C (Lit.[4] 160-162 °C). ^{1}H NMR (400 MHz, $CDCl_3$) δ 8.42 (d, J = 8.6 Hz, 2H, ArH), 8.10 (d, J = 8.6 Hz, 2H, ArH), 7.92 (s, 1H, =CH).

2-(4-methoxybenzylidene) malononitrile (Table 2, Entry 18)

Light yellow solid; m.p. 114.3-114.9 °C (Lit.[8] 113-114 °C). ^{1}H NMR (400 MHz, $CDCl_3$) δ 8.42 (d, J = 8.6 Hz, 2H, ArH), 8.10 (d, J = 8.6 Hz, 2H, ArH), 7.92 (s, 1H, =CH).

3. The NMR spectra for the Knoevenagel condensation products

Ethyl-3-(4-chlorophenyl)-2-cyanoacrylate (Table 2, Entry 1)

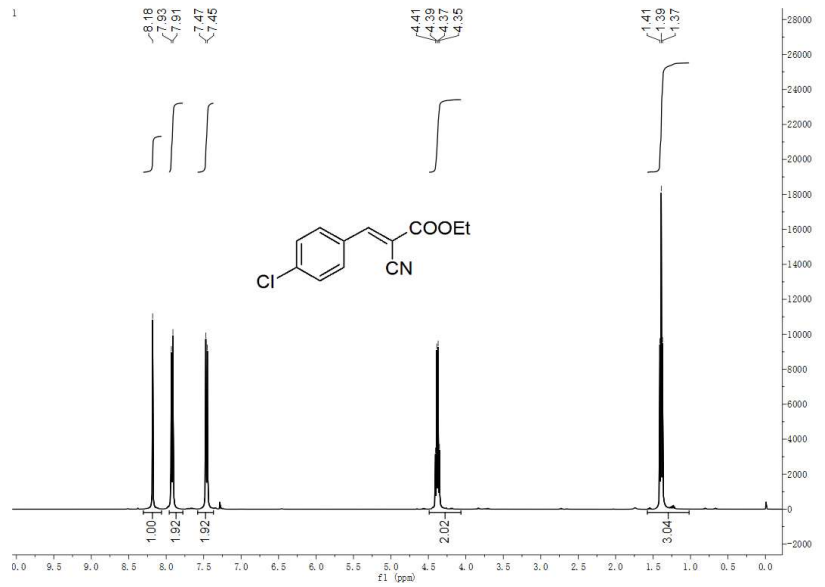

^{1}H NMR spectrum (400 MHz, $CDCl_3$)

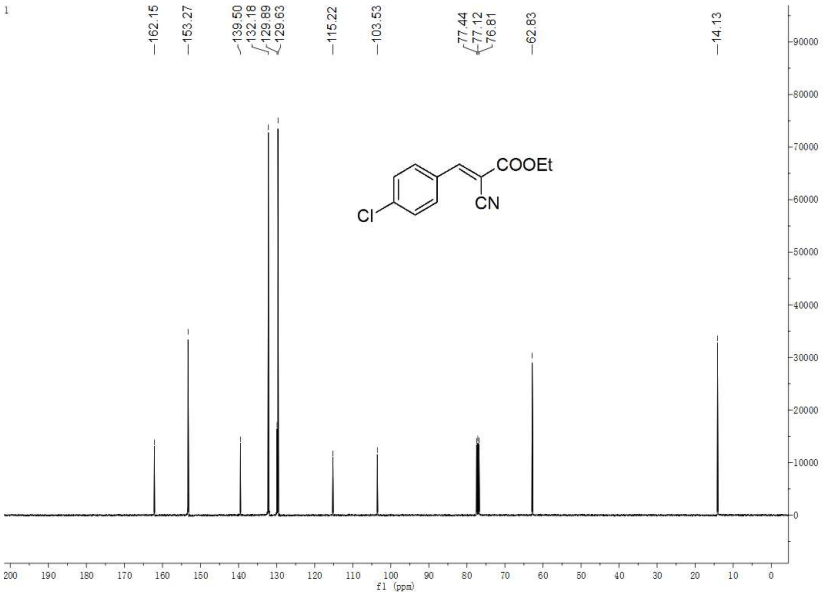

^{13}C-NMR spectrum (101 MHz, $CDCl_3$)

Ethyl-2-cyano-3-(4-nitrophenyl)acrylate (Table 2, Entry 2)

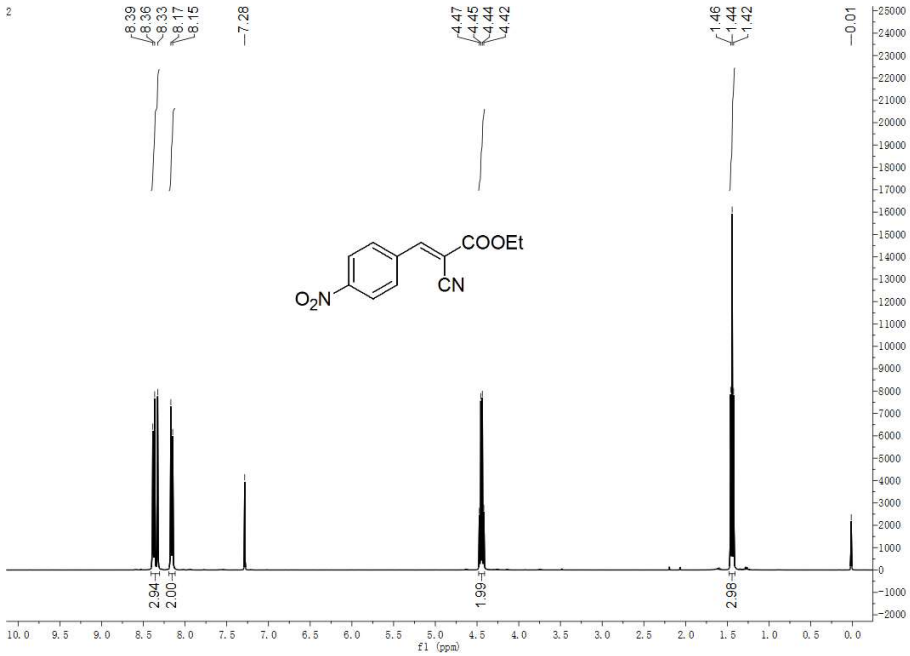

^{1}H NMR (400 MHz, $CDCl_3$)

Ethyl-2-cyano-3-(4-hydroxyphenyl)acrylate (Table 2, Entry 3)

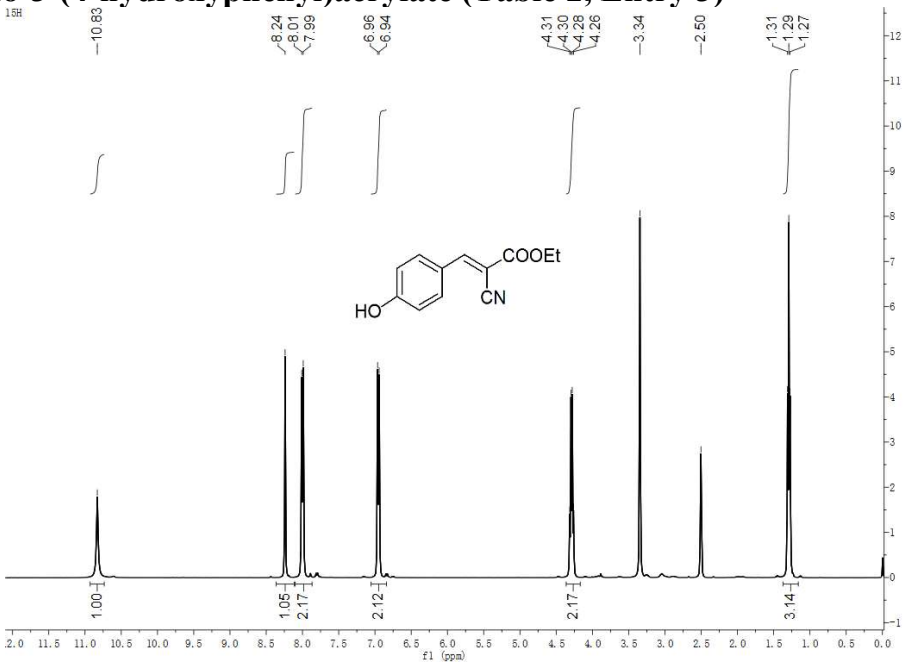

^{1}H NMR (400 MHz, DMSO-d_6)

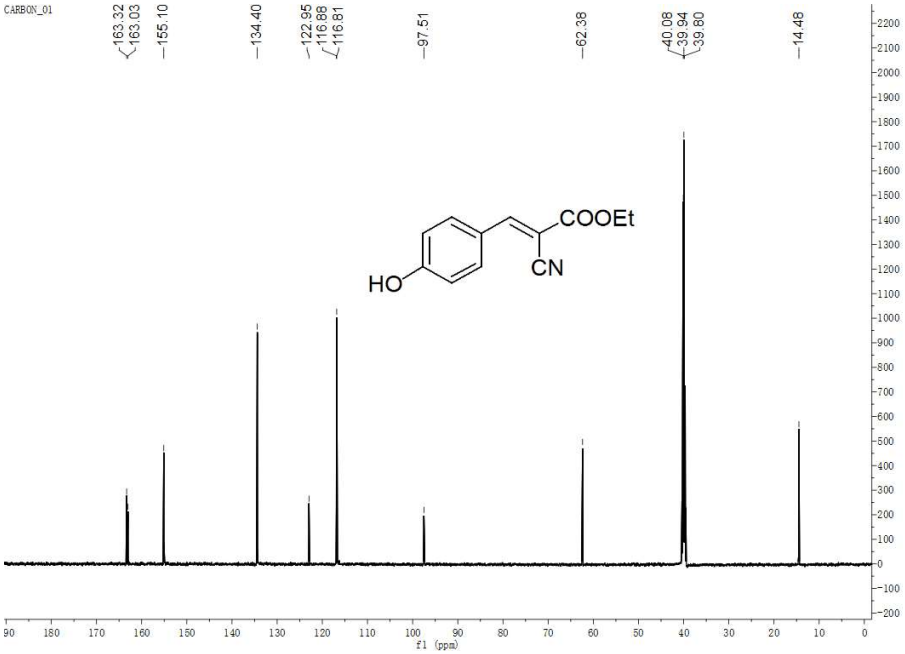

^{13}C-NMR (101 MHz, DMSO-d_6)

Ethyl-2-cyano-3-(4-fluorophenyl)acrylate (Table 2, Entry 4)

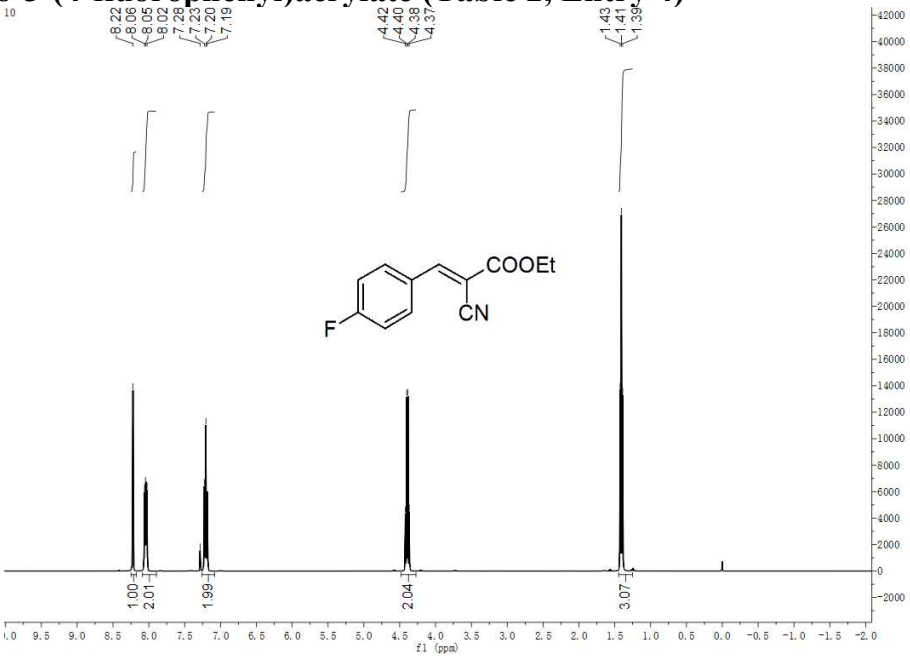

^{1}H NMR (400 MHz, $CDCl_3$)

Ethyl-2-cyano-3-(4-cyanophenyl)acrylate (Table 2, Entry 5)

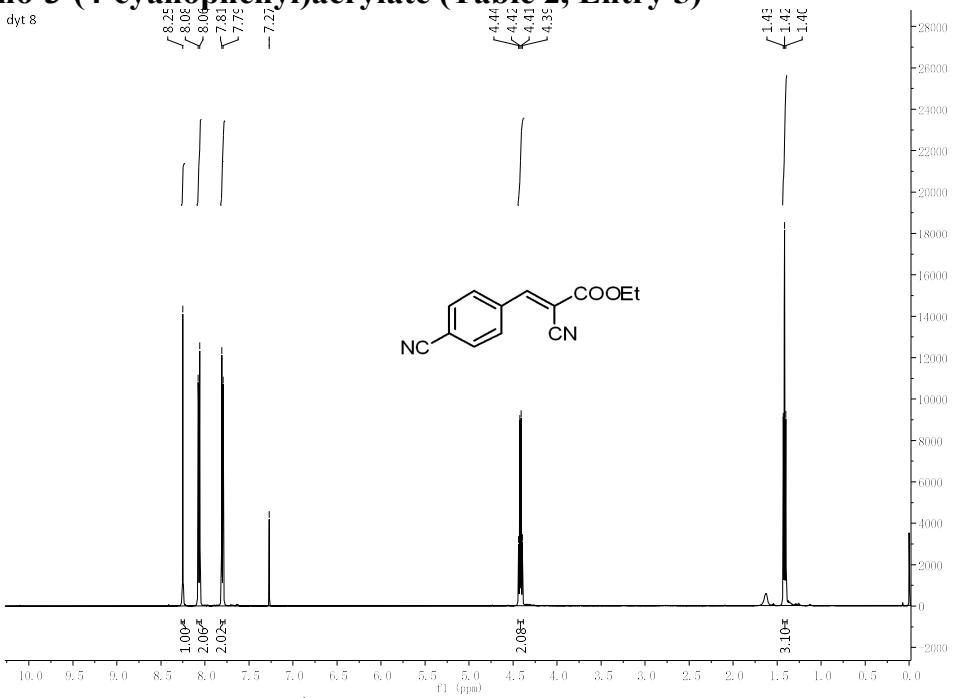

^{1}H NMR (400 MHz, $CDCl_3$)

Ethyl 2-cyano-3-(4-methoxy-phenyl)acrylate (Table 2, Entry 6)

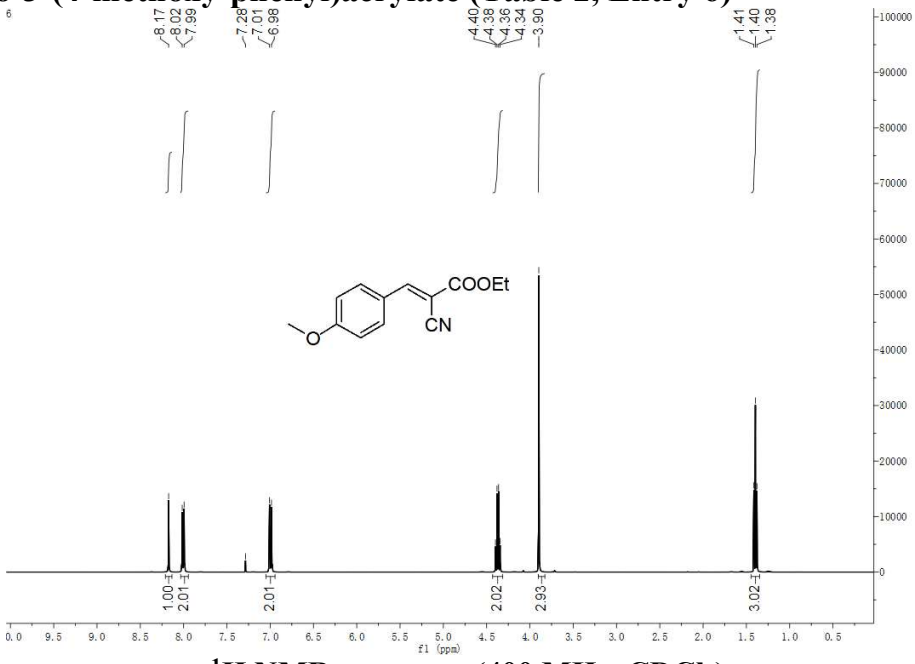

^{1}H NMR spectrum (400 MHz, $CDCl_3$)

Ethyl-2-cyano-3-(4-phenylphenyl)acrylate (Table 2, Entry 7)

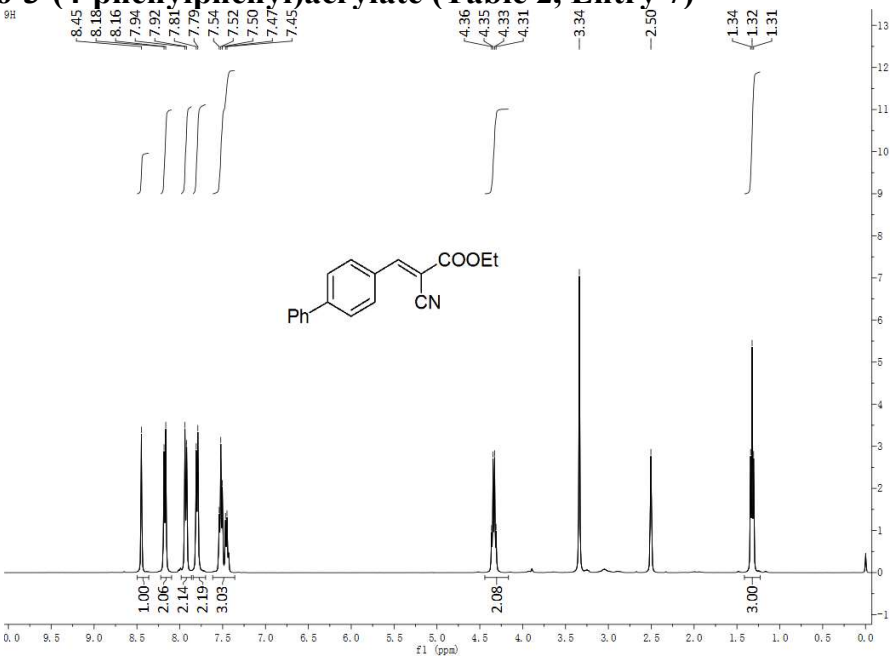

^{1}H NMR (400 MHz, DMSO-d_6)

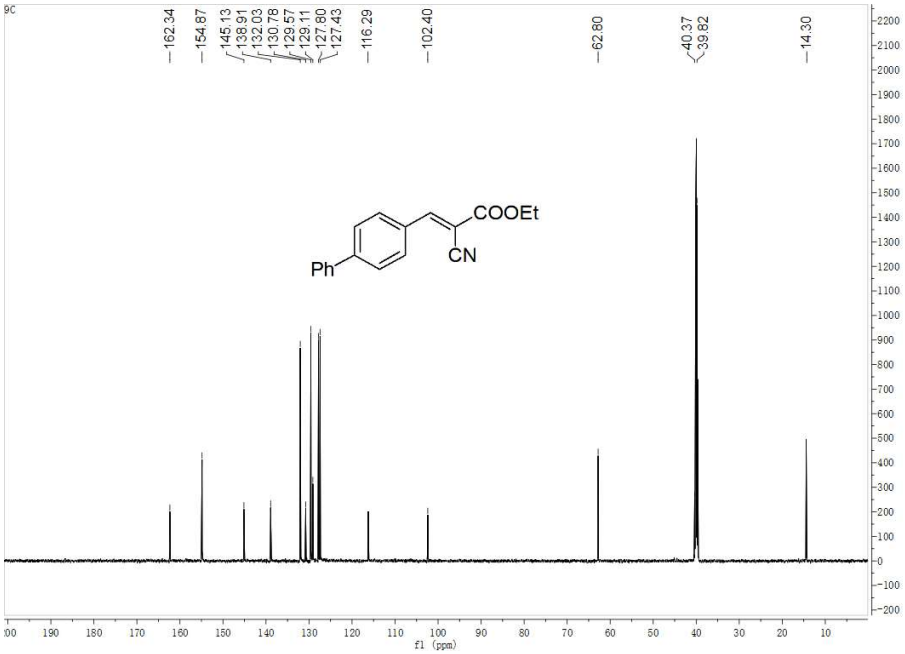

^{13}C NMR (101 MHz, DMSO-d_6)

Diethyl-3, 3'-(1, 4-phenylene)-bis(2-cyanoacrylate) (Table 2, Entry 8)

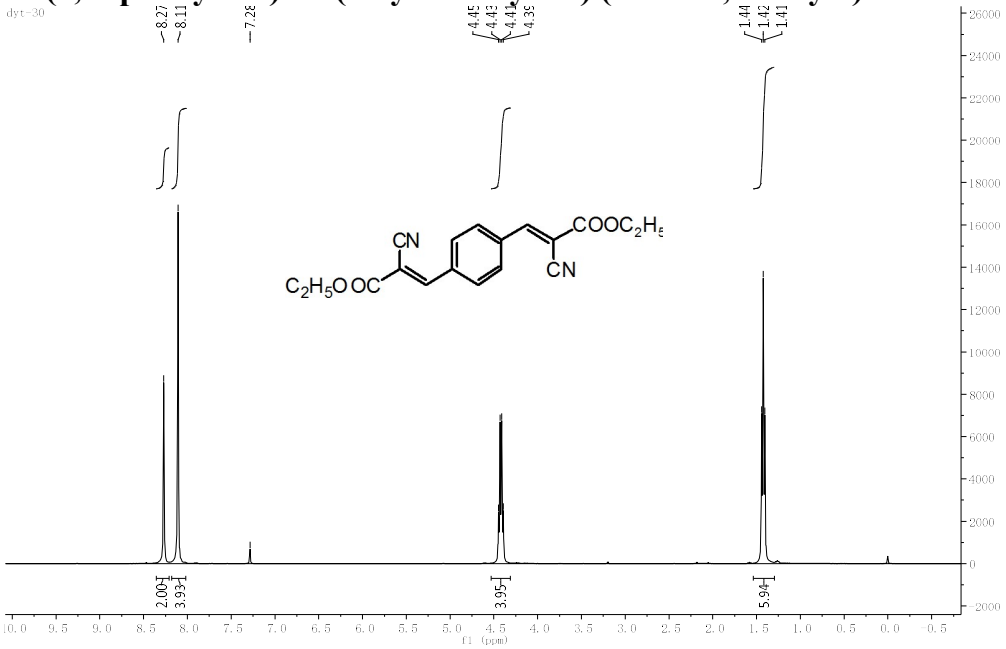

^{1}H NMR spectrum (400 MHz, $CDCl_3$)

Ethyl-2-cyano-3-(2, 4-dichlorophenyl)acrylate(Table 2, Entry 9)

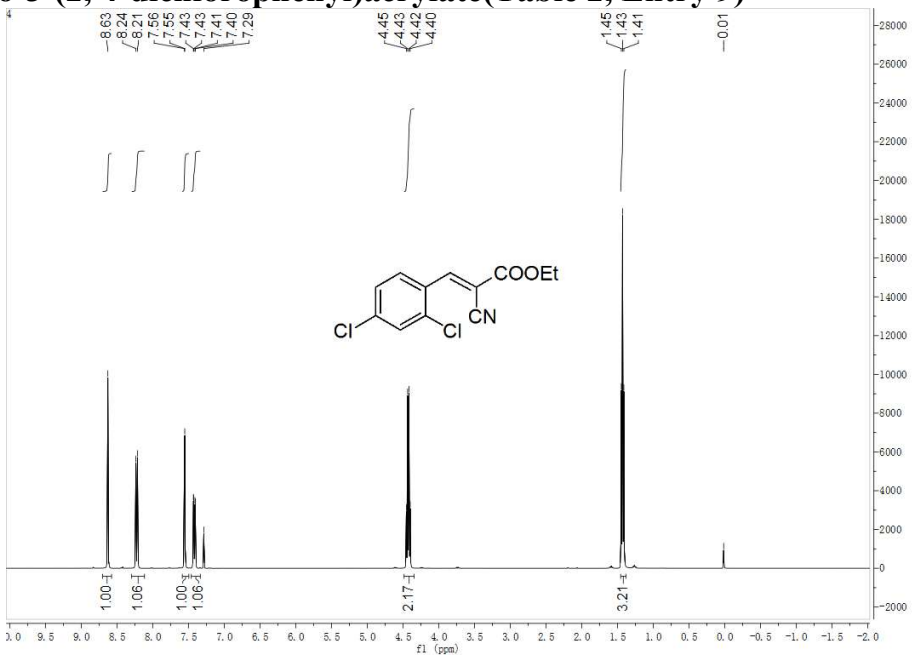

^{1}H NMR spectrum (400 MHz, $CDCl_3$)

Ethyl-2-cyano-3-phenylacrylate (Table 2, Entry 10)

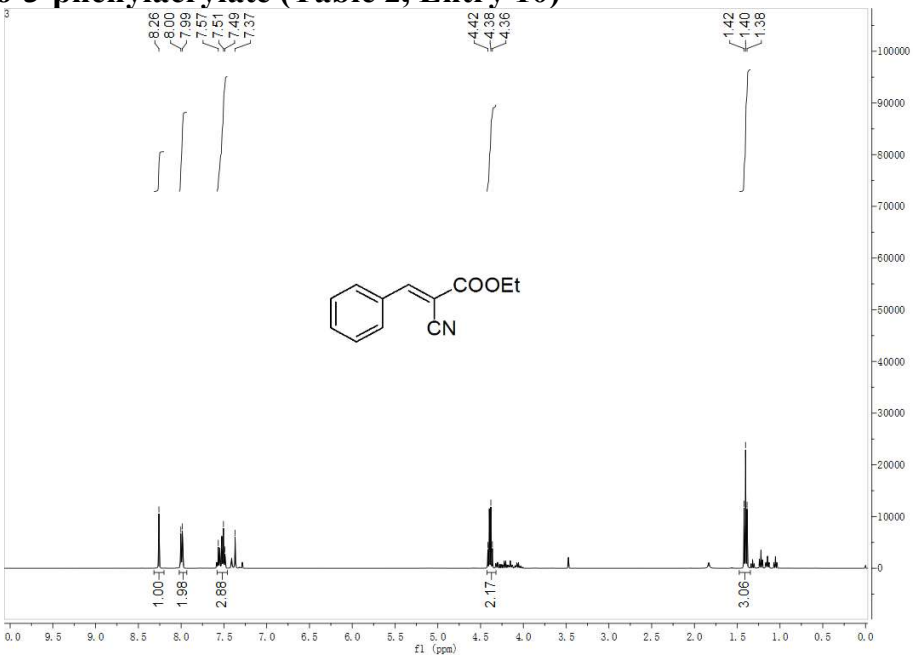

^{1}H NMR spectrum (400 MHz, $CDCl_3$)

Ethyl 2-cyano-3-anthracenylacrylate (Table 2, Entry 11)

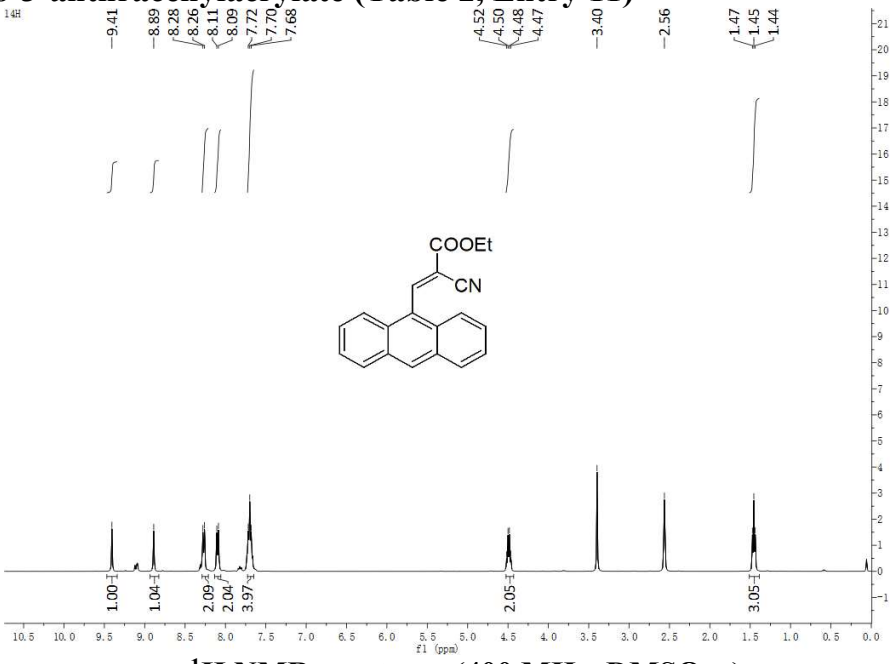

^{1}H NMR spectrum (400 MHz, DMSO-d_6)

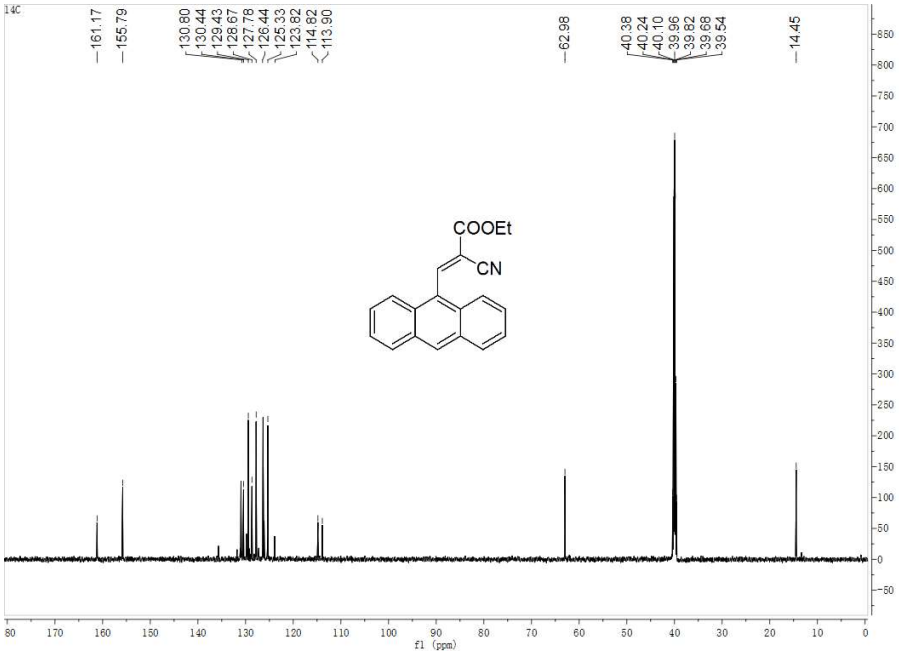

^{13}C NMR spectrum (101 MHz, DMSO-d_6)

Ethyl-2-cyano-3-(2, 4-dimethoxyphenyl)acrylate (Table 2, Entry 12)

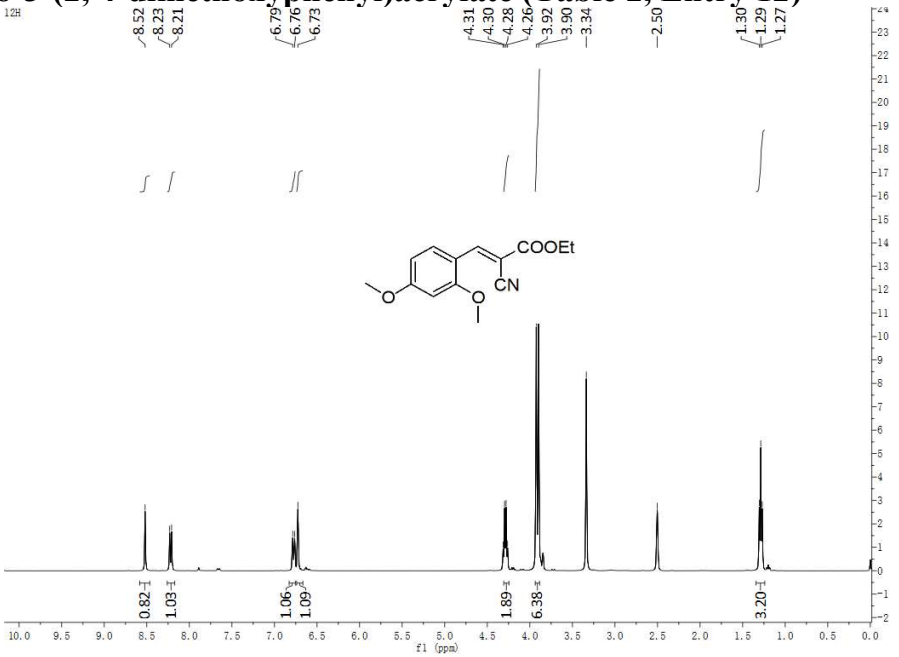

^{1}H NMR spectrum (400 MHz, $CDCl_3$)

Ethyl-2-cyano-3-(2-methoxyphenyl)acrylate (Table 2, Entry 13)

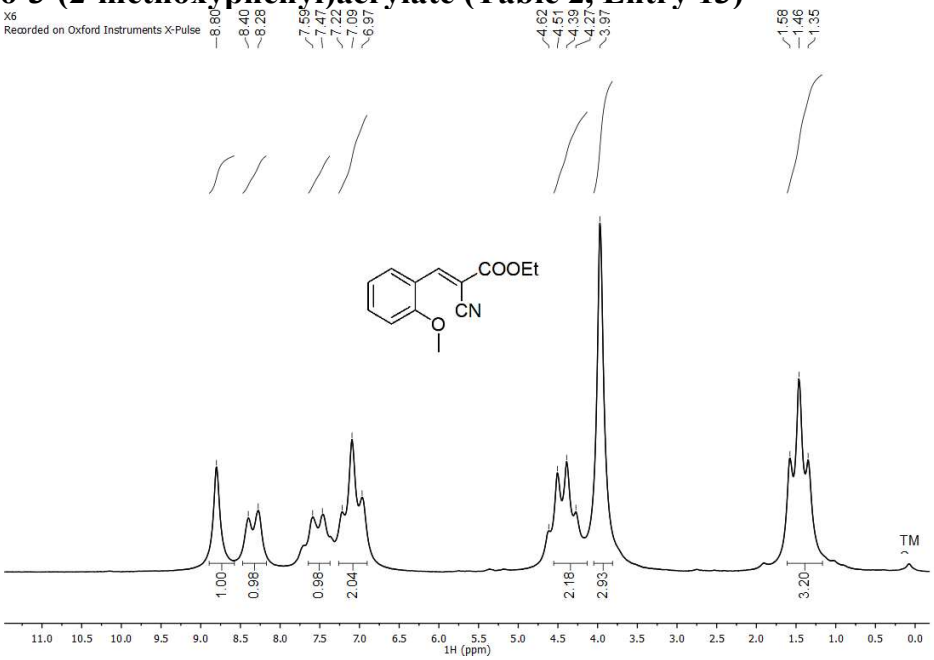

^{1}H NMR spectrum (60 MHz, $CDCl_3$)

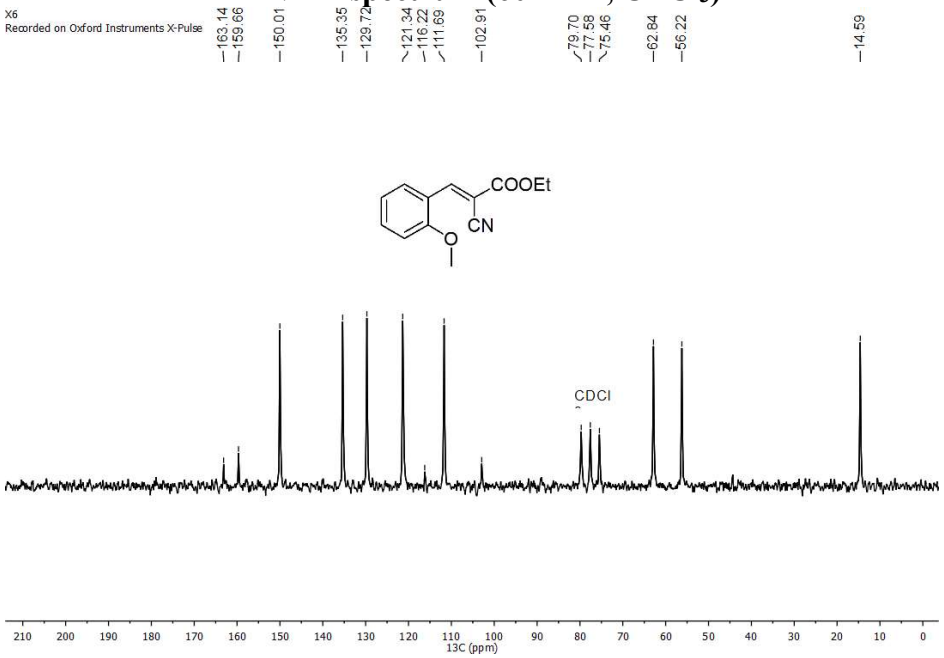

^{13}C NMR (15 MHz, $CDCl_3$)

Ethyl 2-cyano-3-(furan-2-yl)acrylate(Table 2, Entry 14)

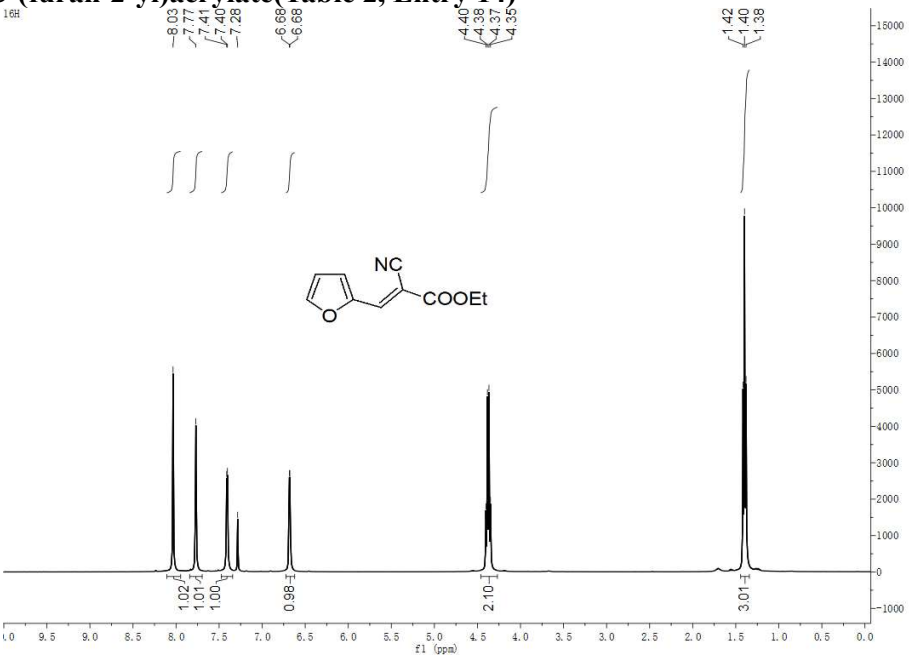

^{1}H NMR spectrum (400 MHz, $CDCl_3$)

Ethyl 2-cyano-3-(*N*-ethylcarbazol-3-yl)acrylate(Table 2, Entry 15)

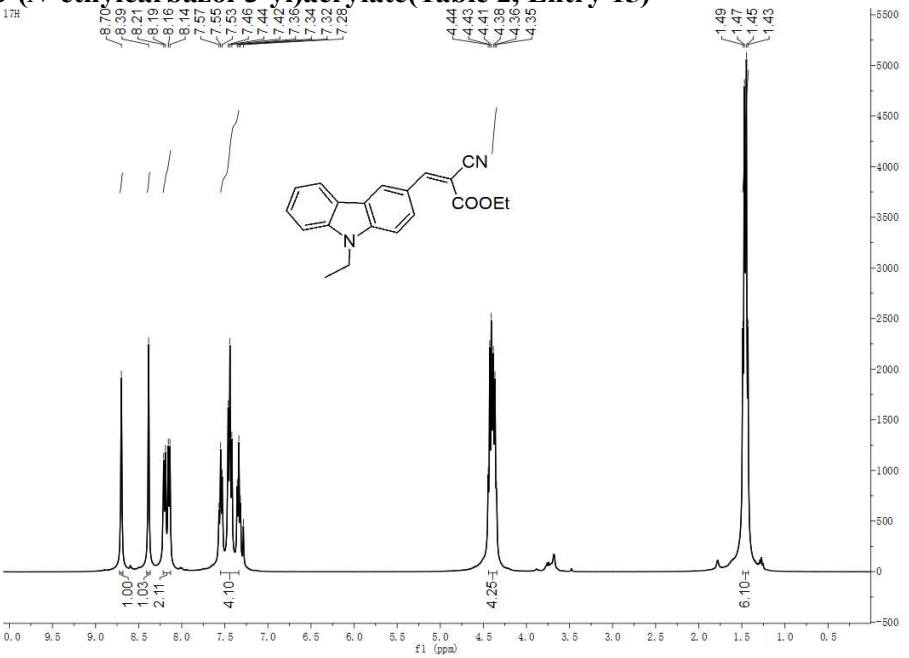

^{1}H NMR spectrum (400 MHz, $CDCl_3$)

2-(4-chlorobenzylidene)malononitrile(Table 2, Entry 16)

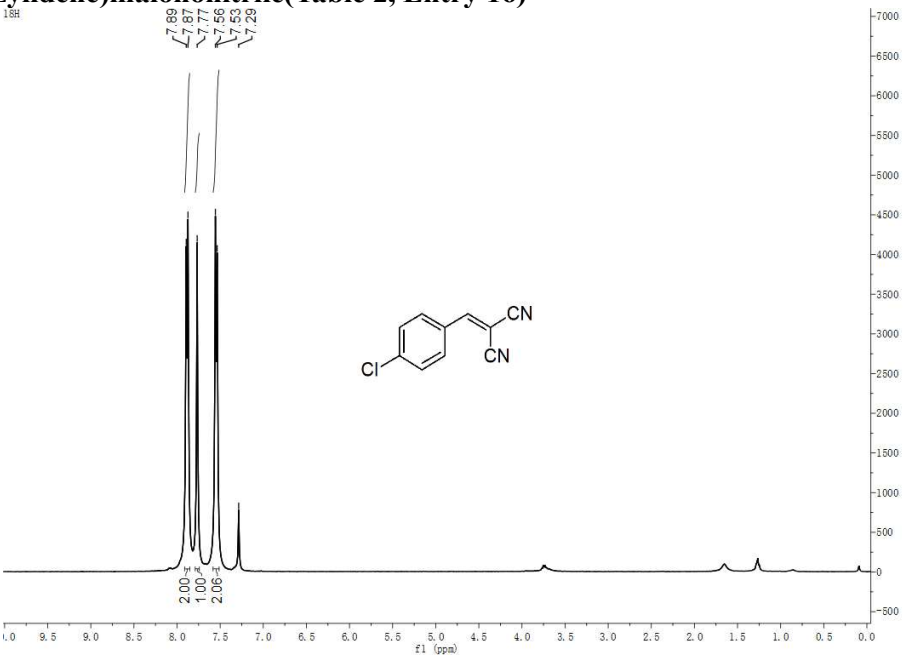

^{1}H NMR spectrum (400 MHz, $CDCl_3$)

3-(4-nitrobenzylidene)malononitrile(Table 2, Entry 17)

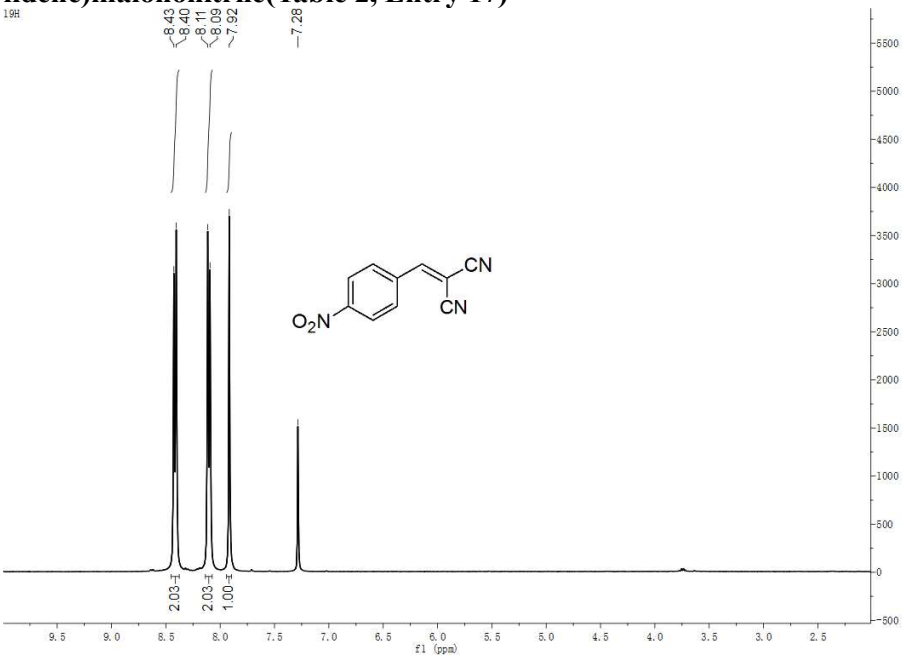

^{1}H NMR spectrum (400 MHz, $CDCl_3$)

2-(4-methoxybenzylidene)malononitrile(Table 2, Entry 18)

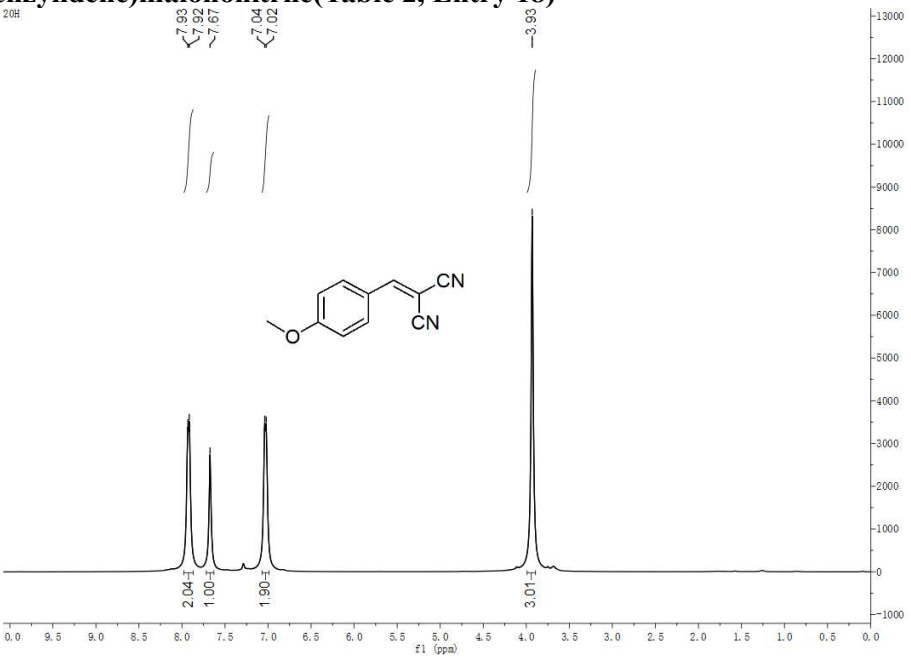

^{1}H NMR spectrum (400 MHz, $CDCl_3$)

4. References

[1] Mahmoud, M. E.; Abdelwahab, M. S.; Fathallah, E. M. Design of Novel Nano-sorbents Based on Nano-magnetic Iron Oxide-Bound-Nano-silicon Oxide-Immobilized-Triethylenetetramine for Implementation in Water Treatment of Heavy Metals. *Chem. Eng. J.* **2013**, *223*, 318–327. DOI: 10.1016/j.cej.2013.02.097.

[2] (a) Kolhatkar, A. G.; Chen, Y. T.; Chinwangso, P.; Nekrashevich, I.; Dannangoda, G. C.; Singh, A.; Jamison, A. C.; Zenasni, O.; Rusakova, I. A.; Martirosyan, K. S.; et al. Magnetic Sensing Potential of Fe_3O_4 Nanocubes Exceeds That of Fe_3O_4 Nanospheres. *ACS Omega.* **2017**, *2*, 8010-8019. DOI: 10.1021/acsomega.7b01312. (b) Ghimire, S.; Dho, J.; Lee, S. G. Tetragonal-Like Distortion and Enhanced Magnetic Anisotropy of the Cubic Spinel Fe_3O_4 Film with a Thin $ZnFe_2O_4$ Capping Layer. *Thin Solid Films* **2020**, *707*, 138073. DOI: 10.1016/j.tsf.2020.138073.

[3] Zhao, S. H.; Meng, D.; Wei, L. L.; Qiao, Y. S.; Xi, F. G. Novel DBU-Based Hydroxyl Ionic Liquid for Efficient Knoevenagel Reaction in Water. *Green Chem. Lett. Rev.* **2019**, *12*, 271–277. DOI: 10.1080/17518253.2019.1637946.

[4] Zhao, S. H.; Zhang, H. R.; Feng, L. H.; Chen, Z. B. Pyridinium Ionic Liquids-Accelerated Amine-Catalyzed Morita-Baylis-Hillman Reaction. *J. Mol. Catal. A: Chem.* **2006**, *258*, 251–256. DOI: 10.1016/j.molcata.2006.05.032.

[5] Heinosuke, Y.; Hiroshi, M. The Knoevenagel Reaction between Hydroxybenzaldehydes and Ethyl Cyanoacetate. *B. Chem. Soc. Jpn.* **1966**, *39*, 1754–1759. DOI: 10.1246/bcsj.

[6] Li, G. W.; Xiao, J.; Zhang, W. Q. Knoevenagel Condensation Catalyzed by a Tertiary-Amine Functionalized Polyacrylonitrile Fiber. *Green Chem.* **2011**, *13*, 1828–1836. DOI: 10.1039/c0gc00877j.

[7] Deshmukh, M. B.; Patil, S. S.; Jadhav, S. D.; Pawar, P. B. Green Approach for Knoevenagel Condensation of Aromatic Aldehydes with Active Methylene Group. *Synth. Commun.* **2012**, *42*, 1177–1183. DOI: 10.1080/00397911.2010.537423.

[8] Ren, Z. J.; Cao, W. G.; Tong, W. Q. The Knoevenagel Condensation Reaction of Aromatic Aldehydes with Malononitrile by Grinding in the Absence of Solvents and Catalysts. *Synth. Commun.* **2002**, *32*, 3475–3479. DOI: 10.1081/SCC-120014780.